



## Constraints on the crustal structure of northern Vietnam based on analysis of teleseismic converted waves

Van-Duong Nguyen<sup>a,b</sup>, Bor-Shouh Huang<sup>c,\*</sup>, Tu-Son Le<sup>b</sup>, Van-Toan Dinh<sup>d</sup>, Lupei Zhu<sup>e</sup>, Kuo-Liang Wen<sup>f</sup>

<sup>a</sup> Taiwan International Graduate Program (TIGP) – Earth System Science Program, Academia Sinica and National Central University, Taiwan

<sup>b</sup> Institute of Geophysics, Vietnam Academy of Science and Technology, Viet Nam

<sup>c</sup> Institute of Earth Sciences, Academia Sinica, Taiwan

<sup>d</sup> Institute of Geological Sciences, Vietnam Academy of Science and Technology, Viet Nam

<sup>e</sup> Department of Earth and Atmospheric Sciences, Saint Louis University, USA

<sup>f</sup> Institute of Geophysics, National Central University, Taiwan

### ARTICLE INFO

#### Article history:

Received 16 January 2013

Received in revised form 23 April 2013

Accepted 26 April 2013

Available online 9 May 2013

#### Keywords:

Receiver function

Crustal thickness

Poisson's ratios

Northern Vietnam

Red River Fault

Bouguer gravity

### ABSTRACT

Here we report estimates of crustal thickness and Poisson's ratios for northern Vietnam, based on teleseismic receiver function analysis of observations from a dense broadband seismic array. The seismic array comprised of 24 stations distributed evenly over northern Vietnam, from whose records we examined 190 teleseismic events of  $M_w > 5.5$  for the period 2006–2008. Using the radial receiver functions calculated from teleseismic records at individual stations, the optimum crustal thickness and  $V_p/V_s$  (where  $V_p$  and  $V_s$  are the velocities of P- and S-waves, respectively) ratio beneath each station were determined using the H- $\kappa$  (where H is crustal thickness and  $\kappa$  is defined as the  $V_p/V_s$  ratio) stacking algorithm. Determined values of crustal thickness range from 26.5 km to 36.4 km, with an average of  $31.0 \pm 2.1$  km. The simple pattern of variation of crustal thickness in the northeastern region of the study area, with a mean of  $\sim 31$  km, suggests that the sector belongs to the craton of the South China block. A highly variable crustal thickness is found over the northwestern region of northern Vietnam, ranging from  $\sim 29.5$  km to  $\sim 36.4$  km, implying that complex tectonic processes have taken place in this region. The thinnest crust is found in the Red River Delta, where it ranges from 26.5 km to 30.4 km, which is suggestive of a recent rifting process. The determinations of crustal thickness show a good linear correlation with Bouguer gravity anomalies. Lower values of Poisson's ratio in the northeastern and Red River Delta sectors suggest a more felsic crust, and larger values in the northwestern sector suggest lithospheric extension in the Song Da depression. The findings enhance our understanding of the geotectonic architecture of the northern Vietnam region.

© 2013 Elsevier B.V. All rights reserved.

### 1. Introduction

The collision between the Indian and Eurasian plates, which was initiated at about 50 Ma, not only resulted in significant deformation within the Tibetan Plateau, but also affected remote areas in Asia (Molnar and Tapponnier, 1975; Tapponnier et al., 1982, 1986, 1990). The 1000-km-long right-slip Red River Fault (RRF) in southernmost China and northern Vietnam is an important structural discontinuity and is mechanically associated with the Indian–Eurasian collision (Allen et al., 1984; Leloup et al., 1995; Leloup et al., 2001). The northern Vietnam region is situated at the southeasternmost extension of the Himalayan syntaxis, and is characterized by several large-scale faults including the RRF, the Dien Bien Phu Fault, and the Ma River Fault (Fig. 1). Knowledge of the crustal structure beneath northern Vietnam is essential to understand how crustal thickening has been

accommodated, and to identify the possible origin of partial melting in the region.

Mantle dynamics and structural evolution in northern Vietnam have been examined with reference to various types of geological and chemical data (Anczkiewicz et al., 2007; Balykin et al., 2010; Findlay, 1997; Findlay and Phan, 1997; Roger et al., 2000; Tran et al., 2008; Wang et al., 1998). Several existing reports regarding the crustal structure of the region are based mainly on gravity data (Bui, 1983; Dang, 2003; Dinh, 2010) and others on magnetotelluric (MT) data (Doan et al., 2000; Le et al., 2008, 2009; Pham et al., 1995). The results derived from these two sets of studies differ considerably because of the problem of non-unique solutions of the potential field. Recently, some seismic studies have been conducted regarding the crustal structure of northern Vietnam (Bai et al., 2010; Dinh, 2010; Huang et al., 2012; Lebedev and Nolet, 2003; Li and van der Hilst, 2010; Starostenko et al., 2009; Wu et al., 2004). However, the resolutions of these studies are relatively low because of the sparse seismic stations or limited profiles covering the study area.

\* Corresponding author. Tel.: +886 2 27839910x323; fax: +886 2 27839871.

E-mail address: [hwbs@earth.sinica.edu.tw](mailto:hwbs@earth.sinica.edu.tw) (B.-S. Huang).

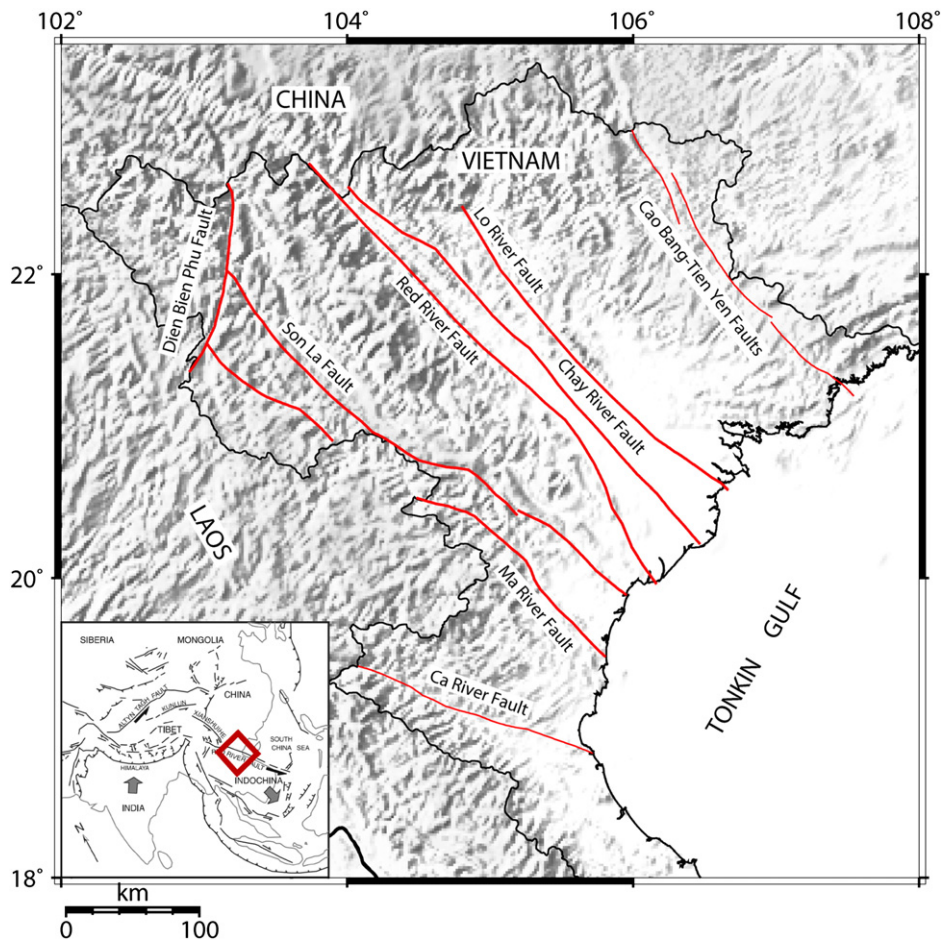


**Fig. 1.** Map of active faults in northern Vietnam. Thick and thin lines represent major and minor active faults, respectively. The panel in the bottom left corner is a sketch regional tectonic map, modified from Gilley et al. (2003).

In a collaborative exercise between the Institute of Geophysics, Vietnam Academy of Science and Technology, and the Institute of Earth Sciences, Academia Sinica, Taiwan, a dense broadband seismic array was installed in northern Vietnam at the end of 2005. These stations are distributed uniformly over the region, and provide a high density of seismic data with a wide dynamic range that enables estimates of the structure of the crust beneath this area (Huang et al., 2009). With the rapid development of broadband seismic networks in recent years, receiver function analysis has become an excellent tool with which to estimate the thickness and  $V_p/V_s$  ratio (where  $V_p$  and  $V_s$  are the velocities of P- and S-waves, respectively) of the crust beneath a seismic array (e.g., Ammon and Zandt, 1993; Owens et al., 1984; Zhu and Kanamori, 2000). In this study, based on the data recorded by this dense seismic array between 2006 and 2008, we report the results of receiver function analysis used to estimate the crustal thickness and Poisson's ratio beneath the seismic stations, and discuss geotectonic aspects of the results including those relating to spatial variations in crustal thickness and to crustal rheology and composition. The observational results of the study are informed by regional geophysical observations and geological data. The findings are expected to improve our understanding of the tectonic evolution of the Indochina Peninsula.

## 2. Regional tectonic setting

Indosinian tectonic movements during the Triassic led to the closure of Paleotethys and caused a reconstruction and reorganization of the continental crust in the area (Dinh, 2010; Le, 1985). The RRF, which is one of the major continental discontinuities in this region,

separates the South China block from the Indochina block and is believed to have had a major impact on the Tertiary tectonic evolution of the region (Anczkiewicz et al., 2007). The RRF is divided into two segments that are characterized by contrasting seismic activity: the northern segment, located in Yunnan, China, records a higher level of seismic activity than the southern segment, which crosses northern Vietnam (Huang et al., 2009). Prior to 32 Ma until about 16 Ma, the RRF was a left-lateral strike-slip lithospheric discontinuity recognized as representing the extrusion of Indochina relative to south China (Leloup et al., 2001). However, evidence for right-lateral strike-slip along the RRF was presented by Leloup et al. (1995, 2001) and Allen et al. (1984), who reported that the sense of movement along the RRF has been oblique right-lateral with a dip component since about 5 Ma. The geodynamic evolution of this area has been closely controlled by the fault systems that have developed since the Mesozoic, and the regional crustal structure in part reflects this deformation.

This study analyzes the northern Vietnam region. Located near the southern segment of the RRF, the region's geotectonic domain includes the southeastern South China terrane and the northern Indochina terrane. The terranes are separated by the NW–SE-trending RRF (Fig. 1). At a regional scale, we divided the study area into four sectors, based on geotectonic characteristics, as follows. (i) The northwestern (NW) sector is bounded by major active faults, including the Ma River Fault, the RRF, and the Dien Bien Phu Fault, and is regarded as the most seismically active zone in Vietnam (Fig. 1). The sector has been folded with fold axes trending NW–SE, and is composed of several geological sub-regions separated by secondary marginal faults. (ii) The northeastern (NE) sector is part of the southeastern South China terrane. Isometric shapes characterize the crustal structures

developed in this sector. (iii) The southeastern end of the RRF of northern Vietnam is a triangular area covered with thick sediment deposited by the Red River, and is named the Red River Delta (RRD) sector in this study. Both the NE and RRD sectors are low-seismicity areas of the study area. (iv) The region south of the Ma River Fault is a stable area of the Indochina block and is named the Truong Son (TS) sector in this study. This sector occupies the most southwestern part of Fig. 1.

### 3. Equipment and observational data

Over a three-year period starting in 2006, 24 broadband seismic stations were installed in northern Vietnam with an inter-station spacing of about 100 km (Fig. 2). Those stations are uniformly spread over the geological sub-regions of northern Vietnam. There are five stations in the NE sector, nine in the NW sector, eight in the RRD sector, and two in the TS sector. These stations are designed to monitor earthquake activity, and provide information to image and interpret crustal and mantle structures beneath northern Vietnam, including the geodynamic evolution of the Red River shear zone (Huang et al., 2009). Each station is equipped with a Nanometrics Trillium 40 broadband sensor and a Quanterra/Kinematics Q330 recorder with 24-bit analog-to-digital conversion. The seismometers measure ground motion over a wide frequency range with a flat response to velocity from at least 0.025 to 50 Hz. The ground motion signal is recorded continuously and digitized at a rate of 100 samples per second. A built-in Global Positioning System (GPS) clock that resets the

internal clock each hour confines timing errors to <1 ms and provides timekeeping for the data.

Seismic events from 2006 to 2008 were selected for this study. We selected 190 teleseismic events (with epicentral distances between 30° and 90°) with  $M_w > 5.5$  to perform the receiver function analysis (Fig. 3). Most of the selected events occurred in the northwestern and southwestern Pacific Ocean, as well as along the Indonesian islands. The selected events provide a good distribution of azimuths for the study area, which allows an average measurement of the crustal structure beneath each station to be obtained. However, the site condition is different for each station and the recording time ranges of several stations are shorter than others for the reason of unstable field supports, the selected record number for each station is changeable and depending on the quality of the recorded data. The number of events per station used in the study varies from 18 to 182 (Table 1) and in average about 75 events per station.

### 4. Analysis

#### 4.1. Calculation of P-wave receiver functions

The teleseismic P-wave coda contains S-waves generated by P–S conversion at the velocity discontinuity between the crust and upper mantle beneath the seismic stations. Receiver functions were obtained by deconvolving the vertical component from the radial and transverse component waveforms of the P-wave coda (Langston, 1979; Li et al., 2008; Owens et al., 1984). Receiver functions at each station were computed according to the following procedure. First, we

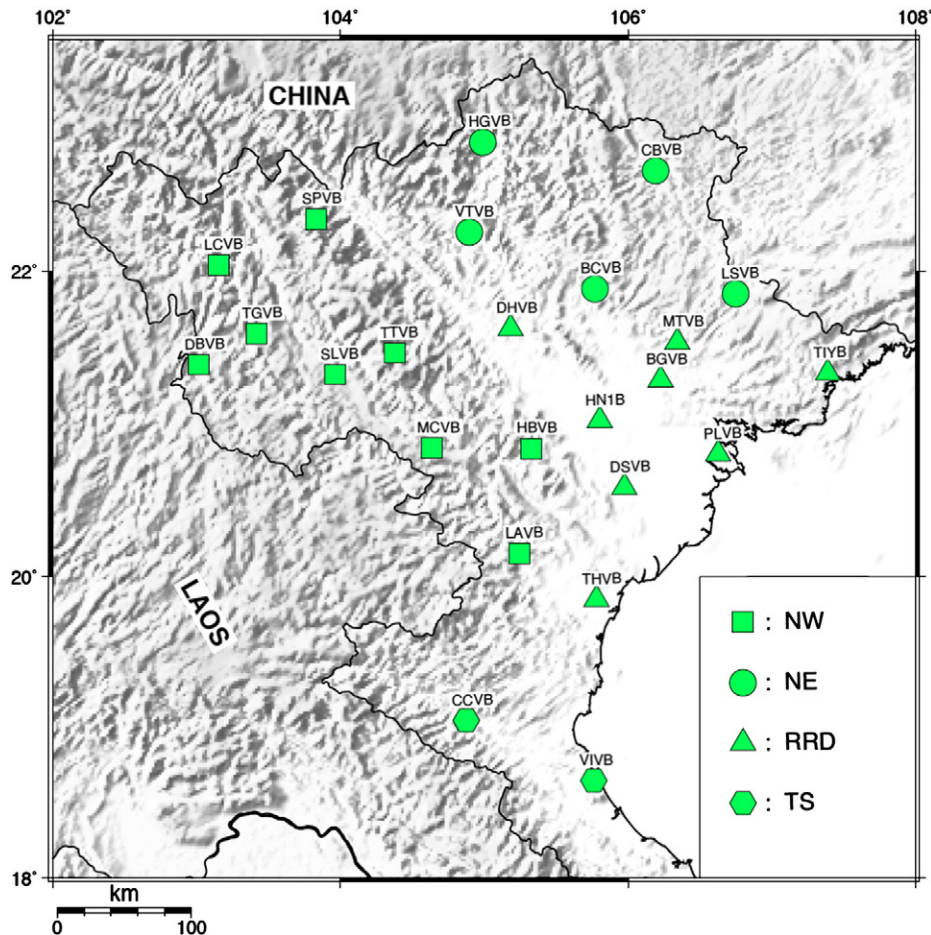
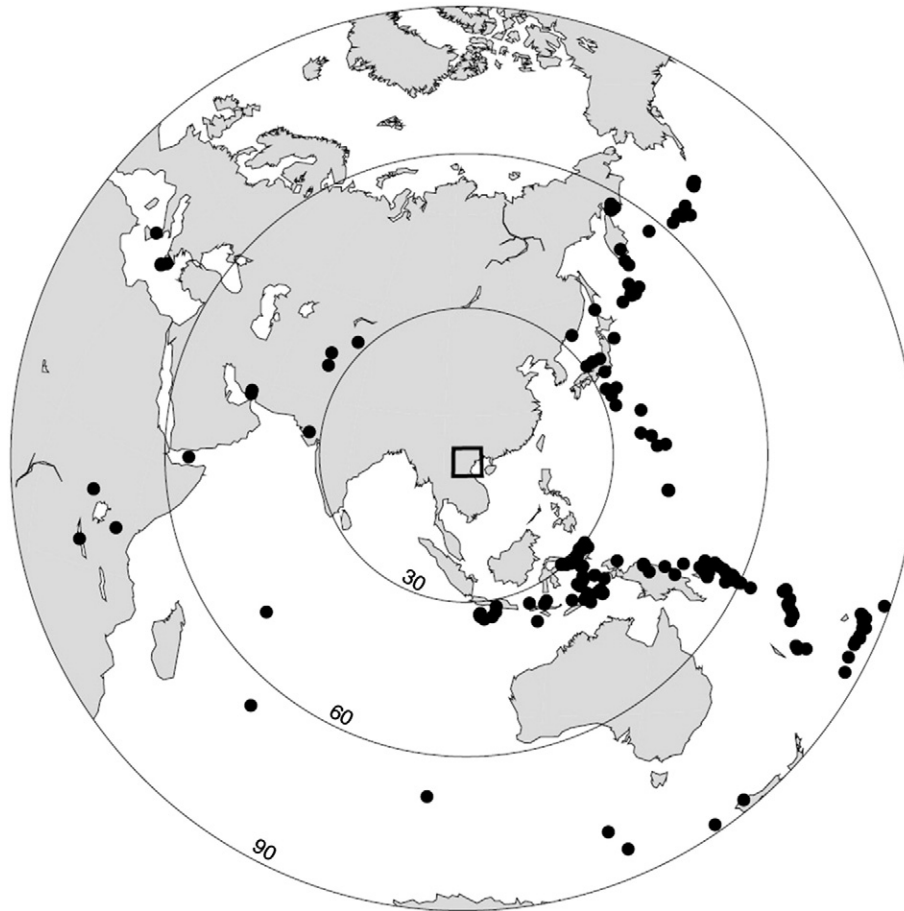


Fig. 2. Map showing the 24 stations of the portable broadband seismic array deployed in northern Vietnam. Four-letter station codes are written in black and listed in Table 1. Each green symbol indicates seismic station group from one of four geotectonic sectors (defined in this study as the NW, NE, RRD, and TS sectors).



**Fig. 3.** Azimuthal projections of epicenters of the 190 earthquakes analyzed in this study (from January 2006 to December 2008), with projection center in northern Vietnam (black rectangle). The epicentral distances range from 30° to 90° for earthquakes with a  $M_w > 5.5$ .

visually checked each event by performing auto- and cross-correlation to ensure that the event had a clear first P-phase and that the recording was of high quality in signal to noise ratio. Noisy recordings were discarded. Second, the selected seismograms were cut from 50 s

before to 150 s after the first P-wave arrivals. The horizontal components were then rotated to the radial and tangential directions and deconvolved with the vertical component in the time domain to estimate the receiver function (Ligorria and Ammon, 1999).

**Table 1**  
Values of crustal thickness,  $V_p/V_s$ , and Poisson's ratio determined in this study. Also given are details about the stations from which seismic data were selected. Uncertainties on the mean values are  $\pm 1\sigma$ .

STA code	Section	Grade	Lat (°)	Lon (°)	Elev (m)	No. of R	tpts (s)	Crustal thickness (km)	$V_p/V_s$	Poisson's ratio ( $\nu$ )
LAVB	NW	A	20.153	105.248	54	94	3.6	29.5 ± 0.9	1.72 ± 0.03	0.245
HBVB	NW	B	20.842	105.328	55	95	3.9	31.5 ± 1.2	1.74 ± 0.04	0.253
MCVB	NW	B	20.844	104.635	826	49	4.5	33.0 ± 0.9	1.82 ± 0.03	0.284
SLVB	NW	B	21.330	103.965	607	93	4.3	32.0 ± 1.0	1.8 ± 0.03	0.277
TTVB	NW	B	21.466	104.379	675	182	4.1	34.6 ± 1.5	1.70 ± 0.05	0.235
DBVB	NW	B	21.39	103.018	480	89	3.8	33.5 ± 1.4	1.68 ± 0.04	0.226
TGVB	NW	A	21.592	103.418	574	118	3.7	31.5 ± 1.3	1.70 ± 0.04	0.235
LCVB	NW	C	22.039	103.155	205	123	4.3	31.4 ± 1.4	1.82 ± 0.05	0.284
SPVB	NW	C	22.338	103.835	1556	73	4.7	36.4 ± 1.3	1.77 ± 0.04	0.266
LSVB	NE	A	21.853	106.749	285	60	3.5	30.0 ± 1.2	1.69 ± 0.04	0.231
BCVB	NE	A	21.885	105.772	51	61	3.6	31.0 ± 1.0	1.69 ± 0.04	0.231
CBVB	NE	B	22.652	106.194	223	38	3.5	32.5 ± 1.1	1.64 ± 0.04	0.204
VTVB	NE	B	22.253	104.899	71	78	3.5	32.5 ± 1.7	1.64 ± 0.04	0.204
HGVB	NE	A	22.836	104.992	119	96	3.9	32.5 ± 1.2	1.72 ± 0.05	0.245
BGVB	RRD	B	21.29	106.228	14	59	3.4	29.4 ± 1.0	1.68 ± 0.04	0.226
DHVB	RRD	C	21.627	105.184	70	18	3.8	29.0 ± 2.0	–	0.269
DSVB	RRD	C	20.587	105.975	88	54	3.5	29.4 ± 2.3	1.70 ± 0.06	0.235
HN1B	RRD	C	21.025	105.804	39	23	3.3	29.0 ± 2.3	1.68 ± 0.08	0.226
MTVB	RRD	A	21.537	106.343	44	42	3.4	30.4 ± 0.8	1.66 ± 0.03	0.215
TIYB	RRD	B	21.335	107.389	37	58	3.3	29.0 ± 1.0	1.67 ± 0.04	0.220
PLVB	RRD	B	20.805	106.628	6	51	3.6	29.9 ± 1.1	1.72 ± 0.03	0.245
THVB	RRD	A	19.851	105.782	1	106	3.2	26.5 ± 1.2	1.72 ± 0.05	0.245
CCVB	TS	B	19.049	104.877	31	37	3.3	31.0 ± 1.2	1.64 ± 0.05	0.204
VIVB	TS	B	18.65	105.763	–6	112	3.1	28.5 ± 1.3	1.66 ± 0.05	0.215

#### 4.2. H– $\kappa$ stacking analysis for crustal thickness and Poisson's ratio

Crustal thickness (H) and  $\kappa$  (defined as the  $V_p/V_s$  ratio) are two key parameters for characterizing the structure and physical properties of the crust (Christensen, 1996). In the receiver function analysis, the primary converted phase Ps and multiple phases (PpPs and PpSs + PsPs) from the Moho discontinuity can be used to estimate values of H and  $\kappa$ , using the H– $\kappa$  stacking algorithm (Zhu and Kanamori, 2000). The H– $\kappa$  domain stack function,  $s(H, \kappa)$ , is defined as

$$s(H, \kappa) = \omega_1 r(t_1) + \omega_2 r(t_2) - \omega_3 r(t_3) \quad (1)$$

where  $r(t)$  is the radial receiver function amplitude and  $t_1$ ,  $t_2$ , and  $t_3$  are the predicted Ps, PpPs, and PpSs + PsPs arrival times. The  $\omega_i$  ( $i = 1, 2, 3$ ) are weighting factors that satisfy  $\omega_1 + \omega_2 + \omega_3 = 1$ . According to both the determined ray parameter and predicted arrival time, the relationship between H and  $\kappa$  is uniquely defined for the Ps, PpPs, and PpSs + PsPs phases (Zhu and Kanamori, 2000). The optimum pair (H,  $\kappa$ ) is the one that yields the maximum stacking amplitude.

Using the radial receiver functions calculated from teleseismic records at individual stations, the optimum crustal thickness and  $V_p/V_s$  ratio beneath each station were determined using the H– $\kappa$  stacking algorithm. The weighting factors  $\omega_1$ ,  $\omega_2$ , and  $\omega_3$  were chosen to equal 0.5, 0.3, and 0.2, respectively, on the basis of the relative amplitudes of P to S converted phases. To perform an H– $\kappa$  stack, it is necessary to specify the average crustal P velocity, for which we used  $V_p = 6.3$  km/s for northern Vietnam for calculating receiver functions and H– $\kappa$  stacking. The uncertainties of crustal thickness and  $V_p/V_s$  ratio were calculated by

$$\sigma_H^2 = 2\sigma_s / \left[ \partial^2 s / \partial H^2 \right] \quad (2)$$

$$\sigma_\kappa^2 = 2\sigma_s / \left[ \partial^2 s / \partial \kappa^2 \right] \quad (3)$$

where  $\sigma_s$  is the estimated variance of  $s(H, \kappa)$  from stacking (Zhu and Kanamori, 2000). The  $V_p/V_s$  ratio ( $\kappa$ ) is uniquely related to the crustal elastic property, Poisson's ratio, defined by

$$\nu = \frac{K^2 - 2}{2(K^2 - 1)}. \quad (4)$$

Poisson's ratio and the  $V_p/V_s$  ratio ( $\kappa$ ) provide much tighter constraints on crustal composition than do either the P- or S-wave velocity alone (Christensen, 1996).

### 5. Results

Receiver functions from clustered events were stacked to increase the signal-to-noise ratio (Fig. 4). We computed a total of 1811 individual receiver functions obtained from 190 events (Fig. 3). To obtain stable results, after many trials, we used a Gaussian parameter of 2.5 to suppress frequencies above 1.25 Hz and down-sampled the waveforms to 10 samples per second. For each station, receiver functions having similar incident angles (i.e., ray parameters, back-azimuth) were averaged. Fig. 4 shows such averaged receiver functions for stations HBVB and HGVB. In general, the transverse receiver functions have small amplitude and no obvious phases at most stations, indicating that there is no clear presence of crustal anisotropy or dipping layers at shallow depths (Bai et al., 2010; Savage, 1998). However, as shown in Fig. 4, some coherent arrivals on the T components (e. g. at about 4 s at HBVB) were observed also, it indicates that the possible crustal anisotropy exists at those stations and provides extra information for detail crustal structure. The converted phases, Ps, and reverberation phases, PpPs, are clearly visible on radial

receiver functions at most of the stations. The phases Ps, PpPs, and PpSs + PsPs lag behind the direct P phase by about 3.1–4.7 s, 11.4–16.0 s, and 14.5–20.8 s, respectively. The quality of the determined receiver function is highly reliant on site conditions. Stations located on basement rocks observed higher-quality data than those situated on alluvial sites did. In one extreme case, the estimated receiver function of station DHVB in the RRD sector (Fig. 2) was overwhelmed by reverberations in the low-velocity sedimentary layer, which induced large errors in the estimation of the  $V_p/V_s$  ratio (Table 1). Hence, we avoided further analysis involving this measurement.

We performed crustal thickness and  $V_p/V_s$  ratio measurements for all 24 stations in northern Vietnam using the H– $\kappa$  domain grid search technique (Zhu and Kanamori, 2000). The estimated crustal thickness and  $V_p/V_s$  ratio beneath each station were obtained from its maximum amplitude in the H– $\kappa$  stack (Fig. 5). The resulting estimates are reported in Table 1, which also contains standard deviation errors, which were calculated based on Eqs. (2) and (3). On the basis of the quality of the original receiver functions, the stations were classified into three grades: A, B, and C (Table 1). The grade A stations (7 in total) display a clear arrival in the time window of 3.0–5.0 s, which is considered as Ps, and at least one of the multiples close to the predicted arrival times (Figs. 4 and 5). For these stations, both the crustal thickness and  $V_p/V_s$  are well resolved with high confidence (Table 1). Grade B stations show clear Ps but not crustal multiples, and the standard deviations of H and  $\kappa$  are  $<1.5$  km and  $<0.05$ , respectively. Twelve stations belong to grade B, for which the results regarding crustal thickness and  $V_p/V_s$  ratio can be used for analysis and interpretation. The Ps phase of receiver functions can be clearly observed at the five stations in grade C, but other crustal phases cannot be identified in the receiver function profiles, and the standard deviations of H and  $\kappa$  in this grade are  $>1.5$  km and  $>0.05$ , respectively (Table 1). The magnitudes of the variations of the estimated H and  $\kappa$  parameters reported in Table 1 are significantly larger than the standard deviations for most of the stations, suggesting that the variations are well constrained. However, it is known that error source can be induced from different choice of the background crust velocity ( $V_p$ ) and the Fresnel zone width of the teleseismic phases may affect data resolution also. These errors must be included and added to the H– $\kappa$  uncertainty. To interpret results based on Table 1, both uncertainties should be considered also.

For the entire study area, the resulting crustal thickness determinations reveal a relatively variable crustal structure. The estimated crustal thickness has an overall mean of 31.0 km, and ranges from 26.5 km in the NE sector to 36.4 km in the NW sector. The resulting  $\kappa$  values vary from 1.64 to 1.82 and have a mean of 1.71, which is lower than the global average of 1.78 for the bulk continental crust (Zandt and Ammon, 1995). Poisson's ratio values, which reflect the spatial variations in physical properties of rocks, vary from 0.204 to 0.284. The distribution of stations across the study area provided an opportunity to examine the spatial variations in both crustal thickness (Fig. 6) and  $V_p/V_s$  ratio (Fig. 7) over the study area, based on the 24 crustal thickness measurements and 23  $V_p/V_s$  ratio determinations. The four sectors defined on the basis of tectonic and geological characteristics are examined in turn below.

The NW sector is regarded as the most active and complex tectonic region in northern Vietnam. The average crustal thickness (H) and  $V_p/V_s$  ratio ( $\kappa$ ) beneath this area are 32.6 km and 1.75, respectively, and  $\nu$  is 0.256 (Table 2). The significant features of this sector are its thicker crust and the higher Poisson's ratios than other sectors (Figs. 6 and 7). This sector can be divided into two sub-sectors on the basis of crustal thickness variations. The first sub-sector (located on the northeastern side of the Son La Fault) is close to the RRF area and has a thick crust (33.9 km on average), with the crust becoming thinner toward the southeast. The second sub-sector is located to the west of the first (Fig. 6). The crust here is slightly thinner, about 32.1 km on average.

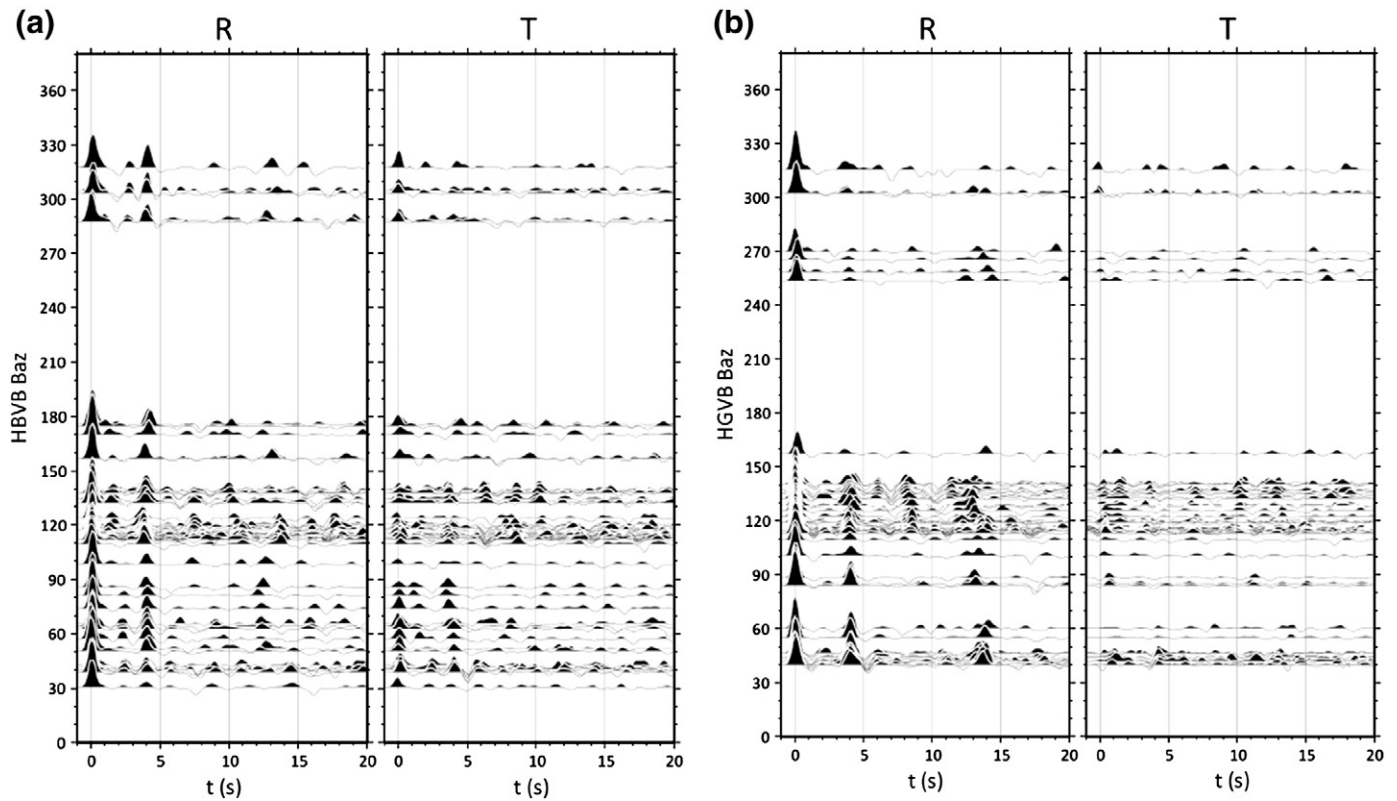


Fig. 4. Radial and transverse components of the receiver functions as a function of back-azimuth at stations (a) HBVB and (b) HGVB. The coherence amplitudes of the transverse component are much smaller than those of the radial component at both stations.

The NE sector is a part of the southeastern South China terrane. This terrane is separated from the Indosinian terrane by the NW–SE-trending RRF. The average crustal thickness and  $V_p/V_s$  ratio are 31.7 km and 1.68, respectively, and  $\nu = 0.223$  (Table 2). The crustal thickness in this sector is fairly uniform, ranging from 30 km to 32.5 km (Table 1 and Fig. 6). The crust is a little thinner in the southeastern part of this sector. Compared with the NW sector, the  $V_p/V_s$  ratios have lower values across the entire sector (Fig. 7).

The RRD sector is tectonically controlled by several deep boundary faults (Fig. 1). The crust beneath the Hanoi plain (a flat region surrounding station HN1B in Fig. 2) is relatively thin, 29 km on average. Crustal thickness varies along a NW–SE trend that runs parallel with the fault system in this zone (Fig. 6). Station DHVB, located at the western extremity of this sector and adjacent to the Red River shear zone, overlies a crust about  $29.0 \pm 2.0$  km thick. The northeastern part of this sector is characterized by a thinner crust. The average  $V_p/V_s$  ratio of  $1.70 \pm 0.06$  for the central plain is slightly higher than the average value of  $1.67 \pm 0.04$  for the northeastern part of the RRD sector, but the crustal thickness values are similar.

The Truong Son (TS) sector to the south has a slightly thicker crust than the RRD sector, and the lowest  $V_p/V_s$  ratio of all the sectors (Tables 1 and 2; Figs. 6 and 7).

## 6. Discussion

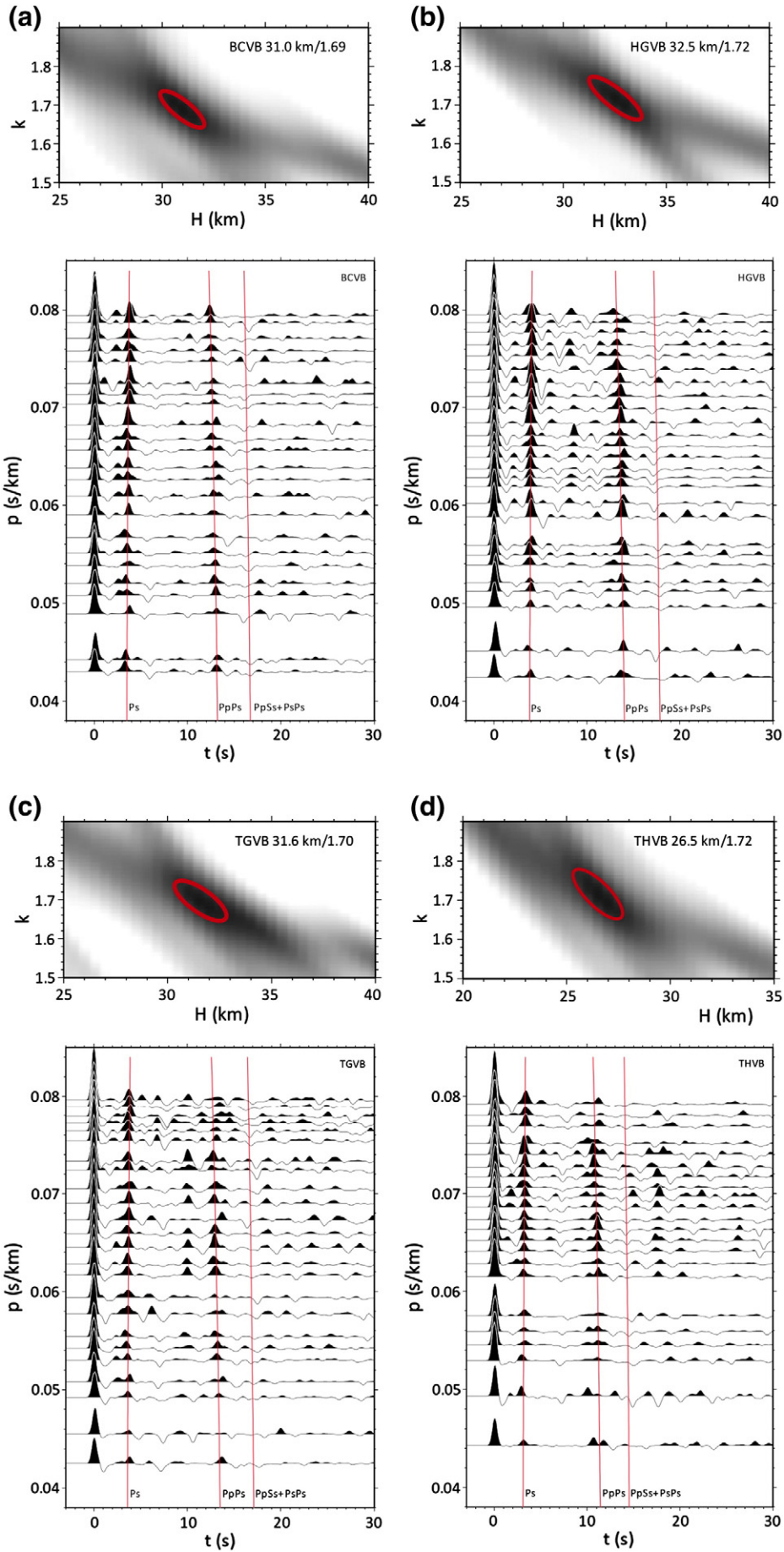
Since 1976, after the reunification of Vietnam, more intensive geophysical surveys have been conducted both onshore and offshore to

determine the crustal structure of northern Vietnam. Until 1980, the map of gravity Bouguer anomalies at a scale of 1:500,000 covered most of the country (Department of Geology and Minerals of Vietnam, 1995). At limited locations in northern Vietnam, some profiles of MT and seismic investigations were also conducted (Doan et al., 2000; Le et al., 2008, 2009; Nguyen, 1996; Pham et al., 1995). These existing geophysical observations can be used to provide a context for the determinations of crustal thickness and Poisson's ratio reported in this study.

To examine the crustal structure of the Red River Fault zone, several MT sounding profiles have been conducted in the past two decades (Doan et al., 2000; Nguyen, 1996; Pham et al., 1995). Nguyen (1996) determined crustal thickness values of 22 km to 30 km along one MT sounding profile, which are consistent with our estimated crustal thickness at station PLVB of 29.9 km. During the period 2007–2008, the first wide-angle reflection/refraction investigations were carried out in North Vietnam along two short profiles (Dinh, 2010). The crustal thickness at station HGVB of 32.5 km determined in this study is consistent with the value of 31.5 km from the seismic sounding by Dinh (2010).

The limited spatial sampling of the previous geophysical observations meant that a two-dimensional (2D) representation of crustal structure in northern Vietnam could not be constructed. To date, the only reliable geophysical data to completely cover the territory of northern Vietnam are gravity anomaly maps (Fig. 8). In the past, therefore, investigations of crustal structure in northern Vietnam relied mainly on gravity data (Bui, 1983; Cao, 1985; Cao and Dinh, 1999; Dang, 2003; Dinh, 2010). Among those investigations, Dang

Fig. 5. Images of the H– $\kappa$  stacking (top) and its receiver functions (bottom) at stations (a) BCVB, (b) HGVB, (c) TGVB, and (d) THVB. Radial receiver functions from each station are arranged as a function of ray parameter with predicted travel times of Ps, PpPs, and PpSs + PsPs (red lines from left to right, respectively). Some clear coherent arrivals do not predicted by red lines are considered as converted waves inside the crust. According to the H– $\kappa$  stacking image, the optimum solution of H and  $\kappa$  is indicated by its peak value in the image and the red ellipse gives a region of its  $1\sigma_H$  and  $1\sigma_\kappa$  uncertainties.



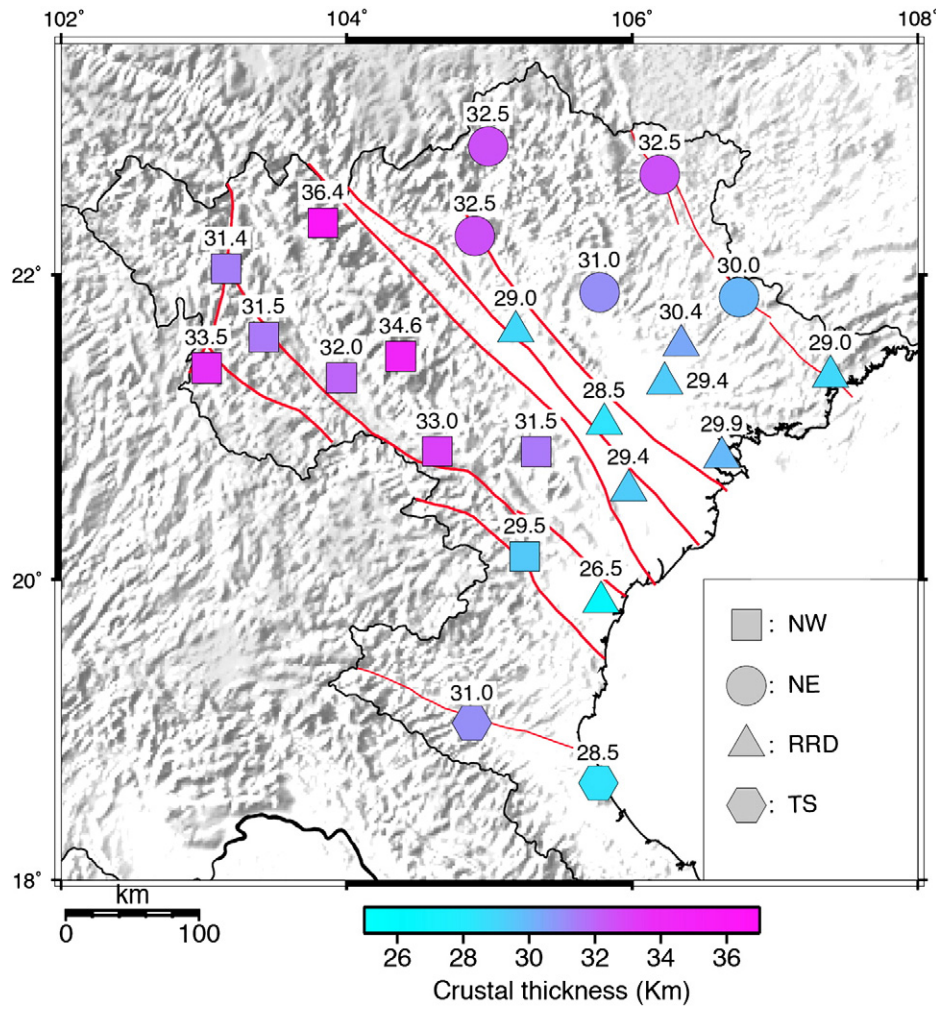


Fig. 6. Values of crustal thickness beneath seismic stations in northern Vietnam. Each symbol defines a group of stations within the same geotectonic sector (Fig. 3).

(2003) constructed a map of the Moho depth for the entire area of northern Vietnam based mainly on a crustal model derived from the interpretation of limited MT profiles, while Dinh (2010) based his crustal model on both MT data and two seismic sounding profiles. Dinh (2010) constructed both Moho and Conrad 2D contour maps for northern Vietnam. Although the results of crustal thickness determined in our study do not constitute a complete 3D surface, our data are well constrained and are evenly distributed across northern Vietnam. Our data provide a good opportunity for comparison with gravity anomaly data and Moho depths from Dang (2003) and Dinh (2010). Fig. 9 shows the relationship between Bouguer gravity anomaly values and Moho depths estimated at the 24 seismic stations. Based on our data, the thick line in Fig. 9 represents the linear relationship for the regression coefficient ( $R$ ) of 0.9 between Moho depths and Bouguer gravity data for northern Vietnam. Our results agree well with previous estimates of Moho depths beneath four stations (DBVB, SPVB, PLVB, and VIVB) from the receiver function analysis of Bai et al. (2010). However, there are large differences between our estimates of crustal thickness and those of Dang (2003) and Dinh (2010). These discrepancies can be explained by the use of different reference crustal models to invert the Moho depths from Bouguer gravity anomalies (Dang, 2003; Dinh, 2010).

In the NE sector, Dang (2003) and Dinh (2010) inverted Moho depths from the gravity data with MT and seismic data to constrain their crustal models, and their results are consistent with the crustal thickness determinations of this study. The combined results show

that the crust in this sector is quite uniform, between 30 km and 32.5 km, as well as similar to the estimates of crustal thickness for the South China block made by Chen et al. (2010) using receiver function analysis. We infer that this sector belongs to the southern margin of the South China fold system, which is a relatively stable tectonic region (Chen et al., 2010). The crust beneath the NE sector also presents a low  $V_p/V_s$  ratio with an average of  $1.68 \pm 0.04$  (Table 2), which suggests that the crust in this sector may be dominantly felsic in composition (Christensen, 1996; Zandt and Ammon, 1995).

The first sub-sector of the NW sector, near the area of the RRF, has a thick crust that thins towards the southeast (Table 1 and Fig. 6). The relatively high  $V_p/V_s$  ratio might be a signature of the active faults, or might be related to metamorphism releasing heat and fluids, or might be reflecting an upwelling of the mantle near the active faults (Le et al., 2008). In the western part of this sector, of this area, the crust is uniformly thick (Fig. 6). This might have resulted from the thinning of the crust and the uplifting process of the mantle that began in the Permian together with the appearance of the NW–SE fault system (Dinh, 2010; Le, 1985). Those processes can be explained by the intra-plate extension and back-arc spreading models (Latin and White, 1990; Nguyen et al., 2008). The high crustal  $V_p/V_s$  ratios of this sector are probably related to lithospheric stretching associated with Permian rifting in the Song Da zone (Balykin et al., 2010). This lithospheric extension resulted in a partial melting of the asthenosphere (Latin and White, 1990; Nguyen et al., 2008), placing the lower crust in a ductile regime (Le et al., 2008). However, this cannot explain the

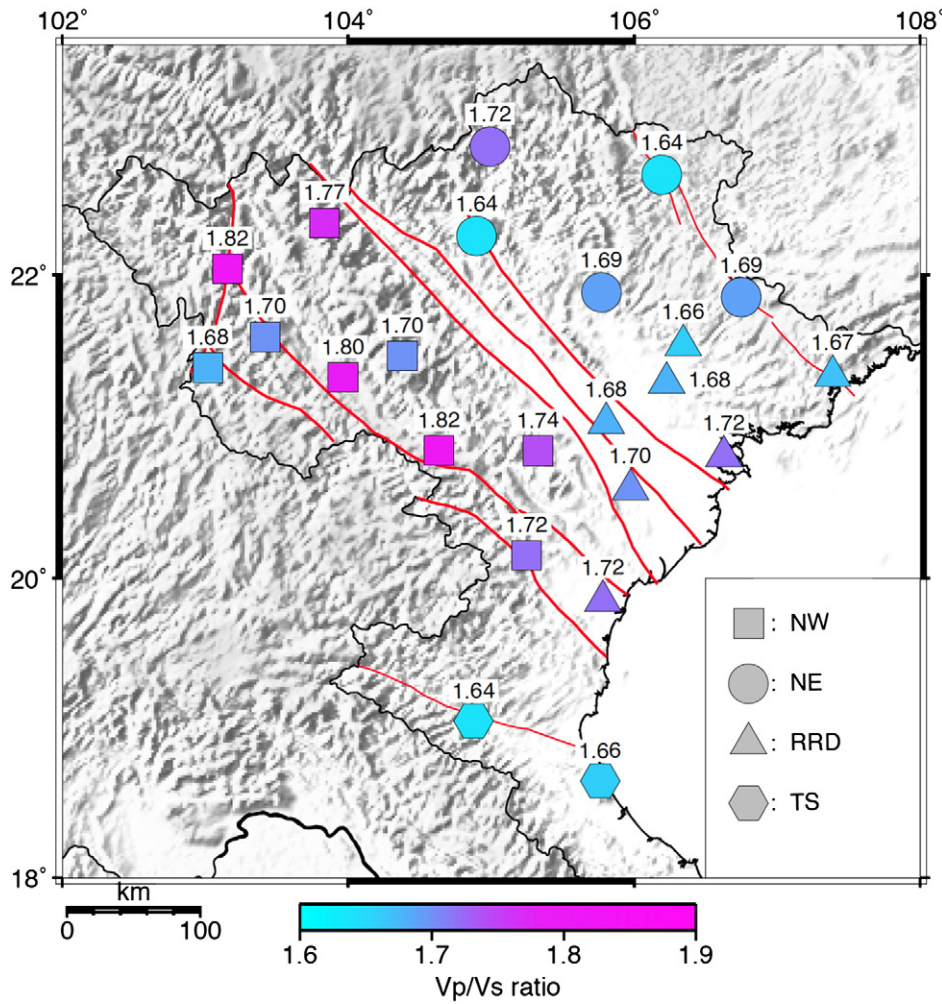


**Fig. 7.** Determined  $V_p/V_s$  ratios beneath seismic stations in northern Vietnam. Each symbol defines a group of stations within the same geotectonic sector (Fig. 3). Station DHVB with a large uncertainty is excluded from this map.

low  $V_p/V_s$  ratios for stations TGVB and DBVB determined in this study (Fig. 7).

The RRD sector, including the Hanoi plain and its eastern coastal plain region, is characterized by a thinner crust and lower  $V_p/V_s$  ratios than in the NW sector. It suggests that the crust in the RRD sector may be dominantly felsic in composition. The Hanoi plain is regarded as an intracontinental rift depression. It is a large-scale superimposed structure formed on the heterogeneous folded basement by rifting in the middle Paleogene (Le, 1985). The thinner crust might have resulted from the lack of crustal loading in this area or the thinning process during the rifting stage, or both. The crustal thickness gradient under the Hanoi plain trends NW–SE, running parallel with the fault system in this zone (Fig. 6). The crustal  $V_p/V_s$  ratio of the Hanoi plain area reveals differences in tectonic situation between

the central part of this sector, and the southern and northern parts (Fig. 7). The relatively high Poisson's ratio for the crust in the central part suggests the impact of geothermal activities in the upper mantle (Dinh, 2010; Tin and Litvinenko, 1986). However, the low  $V_p/V_s$  ratio for the TS sector, in the south of the study area, might be related to a stable cold crust and the lack of mafic or ultramafic igneous rock (Christensen, 1996; Zandt and Ammon, 1995).

In this study, we presented the first report on the crustal structure and Poisson's ratio for northern Vietnam using data from a dense seismic array. These new results constrain the geotectonic architecture of the region. Our results should also contribute significant information for regional seismic wave propagation and hazard reduction across the Indochina Peninsula. However, the results do not have sufficient resolution to quantify the detailed crustal structure across the RRF zone. In this respect, to answer the question about the strain status (lock or creep) in the deep crust of the RRF will require a dense linear array of seismic stations.

**Table 2**  
Average values of parameters of crustal structure for each geo-tectonic sector.

Section	Number of stations	Crustal thickness (km)	$V_p/V_s$	Poisson's ratio ( $\nu$ )
NE	5	$31.7 \pm 1.2$	$1.68 \pm 0.04$	0.223
NW	9	$32.6 \pm 1.2$	$1.75 \pm 0.04$	0.256
RRD	8	$29.0 \pm 1.5$	$1.69 \pm 0.05$	0.230
TS	2	$29.7 \pm 1.2$	$1.65 \pm 0.05$	0.210

## 7. Conclusions

In this study we applied the H– $\kappa$  stacking technique to teleseismic P-wave receiver functions from a 24-station broadband seismic network in northern Vietnam and calculated regional crustal thickness and Poisson's ratio for the region. The results provide new constraints

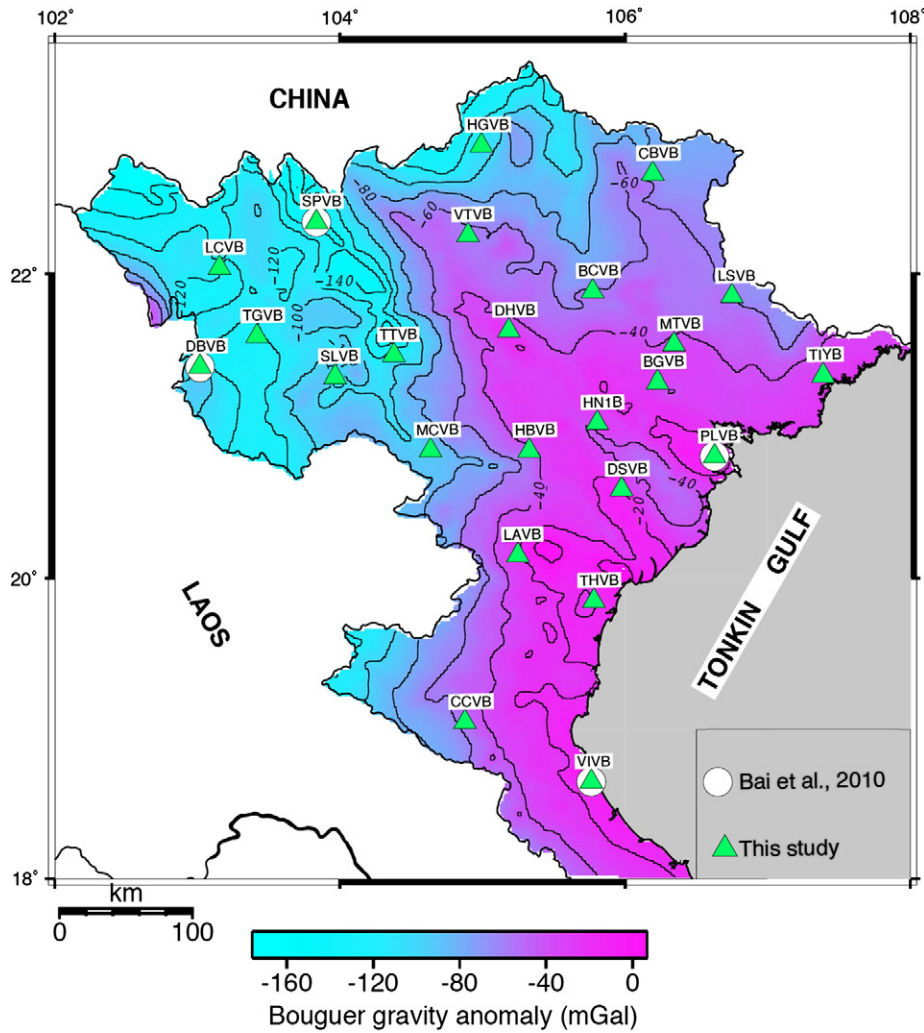


Fig. 8. Bouguer gravity distribution over northern Vietnam (contour interval, 20 mGal). Green triangles and white circles represent the seismic stations for receiver functions analyzed in this study and in the study of Bai et al. (2010), respectively.

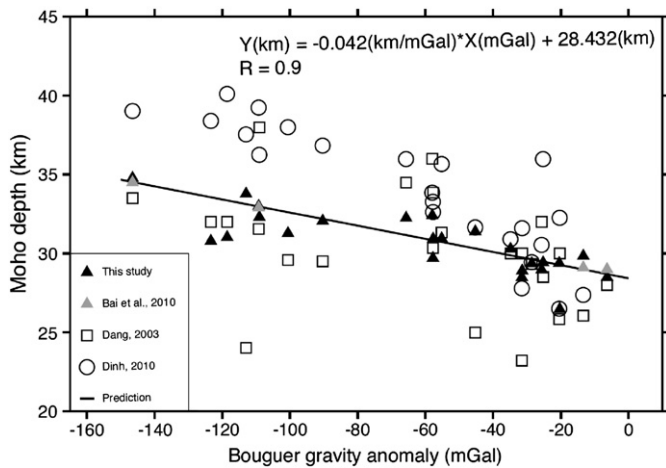


Fig. 9. Comparison of Moho depths beneath seismic stations and corresponding Bouguer gravity anomalies retrieved from the 2D gravity map (Fig. 8). To construct the diagram, each crustal thickness reported in Table 1 has been corrected to the sea level to estimate the Moho depth. The thick black line denotes the linear relationship represented as regression coefficient (R) between the Bouguer gravity anomalies (X) and Moho depths (Y) determined in this study (solid black triangle symbols). Other symbols plot the estimated Moho depths from previous studies at seismic stations (Fig. 8).

on the structure and properties of the crust and on the regional tectonic evolution. Major findings regarding features of the crust and crust–mantle boundary beneath the seismic network include:

- (1) Crustal thickness in northern Vietnam is variable, ranging from 26.5 km to 36.4 km. The Moho interface beneath the NE sector is relatively shallow and uniform, which suggests that this sector is part of the craton platform of the South China terrane. The crustal thickness beneath the RRD sector varies from 26.5 km to 30.4 km. The thin crust of the RRD sector is due to rifting in the South China Sea. A wide variation in crustal thickness is observed across the NW sector, ranging from 29.5 to 36.4 km, implying that this sector has experienced complicated tectonic processes.
- (2) The  $V_p/V_s$  ratio is low in the NE and RRD sectors, about 1.68 and 1.69 on average, respectively. The low values imply that the crustal composition is more felsic than elsewhere. A highly variable  $V_p/V_s$  ratio was found within the NW sector, ranging from 1.68 to 1.82, probably related to extension of the lithosphere in the Song Da depression.
- (3) Our results are consistent with the Moho depths derived from limited previous seismic studies. The estimated depths match well with Bouguer gravity anomalies. However, some discrepancies between our results and previous estimates of Moho depths derived from

Bouguer gravity data may be explained by the characteristics of the models used to invert the Moho to fit the Bouguer gravity anomalies.

## Acknowledgments

We express our appreciation to the staff of the Vietnam Academy of Science and Technology and Academia Sinica for collecting the data used in this study. Dr. H. M. Le provided helpful comments on an earlier draft of the paper. Van-Duong Nguyen was supported by a scholarship of the Taiwan International Graduate Program, Academia Sinica and National Central University, for PhD study. This study was supported by the Vietnam National Foundation for Science and Technology Development (NAFOSTED) under grant 105.04.63.09 and 105.01.24.09, and also by Academia Sinica and the National Science Council, Taiwan, under grants NSC100-2116-M-001-019 and NSC101-2116-M-001-033, respectively.

## References

- Allen, C.R., Gillespie, A.R., Yuan, H., Sieh, K.E., Buchun, Z., Chengnan, Z., 1984. Red River and associated faults, Yunnan Province, China: Quaternary geology, slip rates, and seismic hazard. *Geological Society of America Bulletin* 95, 686–700.
- Ammon, C.J., Zandt, G., 1993. Receiver structure beneath the southern Mojave Block, California. *Bulletin of the Society of America* 83, 737–755.
- Anczkiewicz, R., Viola, G., Müntener, O., Thirlwall, M.F., Villa, I.M., Quong, N.Q., 2007. Structure and shearing conditions in the Day Nui Con Voi massif: implications for the evolution of the Red River shear zone in northern Vietnam. *Tectonics* 26. <http://dx.doi.org/10.1029/2006TC001972> (TC2002).
- Bai, L., Tian, X., Ritsema, J., 2010. Crustal structure beneath the Indochina peninsula from teleseismic receiver functions. *Geophysical Research Letters* 37. <http://dx.doi.org/10.1029/2010GL044874> (L24308).
- Balykin, P.A., Polyakov, G.V., Izokh, A.E., Tran, T.H., Ngo, T.P., Tran, Q.H., Petrova, T.E., 2010. Geochemistry and petrogenesis of Permian ultramafic–mafic complexes of the Jinping–Song Da rift (southeastern Asia). *Russian Geology and Geophysics* 51, 611–624.
- Bui, C.Q., 1983. About the new results of the deep structural study of territory of Vietnam. *Journal of Earth Sciences* T5 (1), 27–40 (in Vietnamese with English abstract).
- Cao, D.T., 1985. The method interpret gravity data to research the Earth's crust of northern Vietnam. *Proceedings of the Second Vietnam Scientific Conference on Geology*. Vietnam Geological Survey, Hanoi 27–40.
- Cao, D.T., Dinh, V.T., 1999. Main crustal feature of the crust in Vietnam and adjacent area on the basic of gravity data. *Proceedings of the Fourth Vietnam National Conference on Marine Science and Technology*, Hanoi, pp. 854–863 (in Vietnamese with English abstract).
- Chen, Y., Niu, F., Liu, R., Huang, Z., Tkalčić, H., Sun, L., Chan, W., 2010. Crustal structure beneath China from receiver function analysis. *Journal of Geophysical Research* 115. <http://dx.doi.org/10.1029/2009JB006386> (B03307).
- Christensen, N.I., 1996. Poisson's ratio and crustal seismology. *Journal of Geophysical Research* 101, 3139–3156. <http://dx.doi.org/10.1029/95JB03446>.
- Dang, T.H., 2003. Study on some characteristics of deep crustal structure and seismotectonic zonation in northern Vietnam. PhD. dissertation, 170 pp. Institute of Geophysics, VAST (In Vietnamese).
- Department of Geology and Minerals of Vietnam, 1995. *Bouguer Gravity Anomaly Map for Northern Vietnam*, Scale 1:500,000. Stored in Northern Geological Mapping Division (Hanoi, Vietnam).
- Dinh, V. T. (2010). Study of the earth crustal structures of Northern Vietnam by using the deep seismic, magnetotelluric investigations and gravity data (eds), Vietnam National Science Project: KC.08.06/06/10: Outcome Report – 8/2010.
- Doan, V.T., Dinh, V.T., Nguyen, T.Y., Nguyen, V.G., 2000. The deep structures and geodynamics of Red River fault zone based on Magnetotelluric data along profile Thanh Son – Thai Nguyen. *Journal of Earth Sciences*, Hanoi 22, 388–398 (In Vietnamese with English abstract).
- Findlay, R.H., 1997. The Song Ma Anticlinorium, northern Vietnam: the structure of an allochthonous terrane containing an early Palaeozoic island arc sequence. *Journal of Asian Earth Sciences* 15, 453–464.
- Findlay, R.H., Phan, T.T., 1997. The structural setting of the Song Ma Region, Vietnam and the Indochina–South China plate boundary problem. *Gondwana Research* 1, 11–33.
- Gilley, L.D., Harrison, T.M., Leloup, P.H., Ryerson, F.J., Lovera, O.M., Wang, J.H., 2003. Direct dating of left-lateral deformation along the Red River shear zone, China and Vietnam. *Journal of Geophysical Research* 108 (B2), 2127. <http://dx.doi.org/10.1029/2001JB001726>.
- Huang, B.S., Le, T.S., Liu, C.C., Dinh, V.T., Huang, W.G., Wu, Y.M., Chen, Y.G., Chang, W.Y., 2009. Portable broadband seismic network in Vietnam for investigating tectonic deformation, the Earth's interior, and early-warning systems for earthquakes and tsunamis. *Journal of Asian Earth Sciences* 36, 110–118.
- Huang, H.H., Xu, Z., Wu, Y.M., Song, X., Huang, B.S., Nguyen, L.M., 2012. First local seismic tomography for Red River Shear Zone, northern Vietnam: stepwise inversion employing crustal P and Pn waves. *Tectonophysics*. <http://dx.doi.org/10.1016/j.tecto.2012.03.030>.
- Langston, C.A., 1979. Structure under Mount Rainier, Washington, inferred from teleseismic body waves. *Journal of Geophysical Research* 84, 4749–4762.
- Latin, D., White, N., 1990. Generating melt during lithospheric extension: pure shear vs. simple shear. *Geology* 18, 327–331.
- Le, D.B., 1985. Structure of Vietnam and stages of its formation – on the background of SE Asia. PhD. dissertation abstract, 36 pp. Hanoi National Library, Hanoi (In Vietnamese).
- Le, H.M., Vo, T.S., Nguyen, C.T., Nguyen, T.V., Nguyen, D.X., Marquis, G., Tran, V.T., 2008. Two dimensional electrical structure of the Son La fault zone on the results of magnetotelluric sounding. *Journal of Earth Sciences*, Hanoi 30, 491–502 (In Vietnamese with English abstract).
- Le, H.M., Pham, V.N., Boyer, D., Nguyen, N.T., Le, T.T., Nguyen, V.Q., Marquis, G., 2009. Investigation on the deep geoelectric structure of the Lai Chau–Dien Bien fault zone by magnetotelluric sounding. *Journal of Geology*, Hanoi A/311, 11–21 (In Vietnamese with English abstract).
- Lebedev, S., Nolet, G., 2003. Upper mantle beneath Southeast Asia from S velocity tomography. *Journal of Geophysical Research* 108 (B1), 2048. <http://dx.doi.org/10.1029/2000JB000073>.
- Leloup, P.H., Lacassin, R., Tapponnier, P., Scharer, U., Zhong, D., Liu, X., Zhang, L., Ji, S., Phan, T.T., 1995. The Ailao Shan–Red River shear zone (Yunnan, China), Tertiary transform boundary of Indochina. *Tectonophysics* 251, 3–84.
- Leloup, P.H., Arnaud, N., Lacassin, R., Kienast, J.R., Harrison, T.M., Phan, T.T., Replumaz, A., Tapponnier, P., 2001. New constraints on the structure, thermochronology, and timing of the Ailao Shan–Red River shear zone, SE Asia. *Journal of Geophysical Research* 106, 6683–6732. <http://dx.doi.org/10.1029/2000JB000322>.
- Li, C., van der Hilst, R.D., 2010. Structure of the upper mantle and transition zone beneath Southeast Asia from traveltimes tomography. *Journal of Geophysical Research* 115. <http://dx.doi.org/10.1029/2009JB006882> (B07308).
- Li, Y., Wu, Q., Zhang, R., Tian, X., Zeng, R., 2008. The crust and upper mantle structure beneath Yunnan from joint inversion of receiver functions and Rayleigh wave dispersion data. *Physics of the Earth and Planetary Interiors* 170, 134–146.
- Ligorria, J.P., Ammon, C.J., 1999. Iterative deconvolution and receiver-function estimation. *Bulletin of the Seismological Society of America* 89, 1395–1400.
- Molnar, P., Tapponnier, P., 1975. Cenozoic tectonics of Asia: effects of a continental collision. *Science* 189, 419–426.
- Nguyen, T. K. T., (1996). Underground water exploration in Cuu Long and Red River deltas using magnetotelluric and geoelectrical methods (eds). Vietnam National Basic Science Project: Outcome Report–1996, 446 pp.
- Nguyen, H., Nguyen, D.L., Nguyen, V.C., 2008. Petrogenesis and mantle dynamics of Palaeozoic volcanism in the Song Da structure. *Journal of Geology*, Hanoi B/31–32, 313–330.
- Owens, T.J., Zandt, G., Taylor, S.R., 1984. Seismic evidence for an ancient rift beneath the Cumberland Plateau, Tennessee: a detailed analysis of broadband teleseismic P-wavesforms. *Journal of Geophysical Research* 89, 7,783–7,795.
- Pham, V.N., Boyer, D., Nguyen, V.G., Nguyen, T.K.T., 1995. Electrical properties and deep structure of the Red River fault zone in North Vietnam from magnetotelluric sounding results. *Comptes Rendus. Académie des Sciences* 320 (IIa), 181–187.
- Roger, F., Leloup, P.H., Jolivet, M., Lacassin, R., Phan, T.T., Brunel, M., Seward, D., 2000. Long and complex thermal history of the Song Chay metamorphic dome (Northern Vietnam) by multi-system geochronology. *Tectonophysics* 321, 449–466.
- Savage, M., 1998. Lower crustal anisotropy or dipping boundaries: effects on receiver functions and a case study in New Zealand. *Journal of Geophysical Research* 103, 15069–15087.
- Starostenko, V., Cao, D.T., Pham, N.H., Le, V.D., Nguyen, X.B., 2009. Some outlines of the Vietnamese lithosphere structure on the basis of seismic tomography and satellite gravity data. *Journal of Geology*, Hanoi A/314, 9–17 (In Vietnamese with English abstract).
- Tapponnier, P., Peltzer, G., Le Dain, A.Y., Armijo, R., Cobbold, P., 1982. Propagating extrusion tectonics in Asia: new insights from simple experiments with plasticine. *Geology* 10, 611–616.
- Tapponnier, P., Peltzer, G., Armijo, R., Coward, M.P., Ries, A.C., 1986. On the mechanics of the collision between India and Asia. *Collision Tectonics*. : 19. Geological Society Special Publication, pp. 115–157.
- Tapponnier, P., Lacassin, R., Leloup, P.H., Scharer, U., Zhong, D., Wu, H., Liu, X., Ji, S., Zhang, L., Zhong, J., 1990. The Ailao Shan/Red River metamorphic belt: Tertiary left-lateral shear between Indochina and South China. *Nature* 343, 431–437.
- Tin, H.L., Litvinenko, O.K., 1986. The structure of the earth's crust of the Hanoi trough according to geophysical data and the problem of its riftogenesis. *Journal of Geodynamics* 5, 179–203.
- Tran, T.H., Izokh, A.E., Polyakov, G.V., Borisenko, A.S., Tran, T.A., Balykin, P.A., Ngo, T.P., Rudnev, S.N., Vu, V.V., Bui, A.N., 2008. Permo-Triassic magmatism and metallogeny of Northern Vietnam in relation to the Emeishan plume. *Russian Geology and Geophysics* 49, 480–491.
- Wang, P., Lo, C., Lee, T., Chung, S., Lan, C., Nguyen, T.Y., 1998. Thermochronological evidence for the movement of Ailao Shan–Red River shear zone: a perspective from Vietnam. *Geology* 26, 887–889.
- Wu, H.H., Tsai, Y.B., Lee, T.Y., Lo, C.H., Hsieh, C.H., Dinh, V.T., 2004. 3-D shear wave velocity structure of the crust and upper mantle in South China Sea and its surrounding regions by surface wave dispersion analysis. *Journal of the Marine Geophysical Researches* 25, 5–27. <http://dx.doi.org/10.1007/s11001-005-0730-8>.
- Zandt, G., Ammon, C.J., 1995. Continental crust composition constrained by measurements of crustal Poisson's ratio. *Nature* 374, 152–154. <http://dx.doi.org/10.1038/374152a0>.
- Zhu, L., Kanamori, H., 2000. Moho depth variation in southern California from teleseismic receiver functions. *Journal of Geophysical Research* 105, 2969–2980.